

Source study of M_w 5.4 April 4, 2011 India–Nepal border earthquake and scenario events in the Kumaon–Garhwal Region

Himanshu Mittal¹  · Ashok Kumar² · Yih-Min Wu^{1,3} · Kamal⁴ · Arjun Kumar⁵

Received: 7 August 2014 / Accepted: 20 January 2016 / Published online: 21 April 2016
© Saudi Society for Geosciences 2016

Abstract In the present work, ground motion is estimated from future scenario earthquakes at different sites in Uttarakhand Himalayas in India using empirical Green's function (EGF) technique. The recorded ground motion from April 4, 2011, M_w 5.4 earthquake is taken as a basic element. The ground motion is estimated at 24 sites, where the element earthquake was recorded. It is observed from synthesized time histories that sites located near the epicenter may expect accelerations in excess of 1 g. In the present analysis, Dharchula can expect ground accelerations in excess of 1 g. For M_w 7.0, the expected peak values of acceleration (A_{max}) and velocity (V_{max}) on horizontal components at different sites range between 11 and 912 gal and 5 and 52 cm/s, respectively. The corresponding values for the Z component range between 8 and 228 gal, and 3 and 14 cm/s, respectively. Similarly, for M_w 7.5, the expected A_{max} and V_{max} on horizontal components at different sites range between 25 and 1281 gal and 25 and 102 cm/s, respectively. The corresponding values for the Z component range between 14 to 474 gal, and 15 to 70 cm/s,

respectively. The site amplification functions are estimated using the horizontal-to-vertical spectral ratio procedure. Zone IV (on a scale of II to V according to the seismic zonation map for India) response spectrum for 5 % damping is deficient for M_w 7.0, while zone V response spectrum is exceeded at several frequencies for same magnitude. For M_w 7.5, zone IV response spectrum is conservative (except at some frequencies), while zone V response spectrum is exceeded at many sites. The estimated PGA values can be incorporated in marking the weak areas in the central Himalaya, thereby assisting the designing and construction of new structures.

Keywords Uttarakhand Himalayas · EGF · PGA · Response spectra · RVT

Introduction

Continuing collision between the Indian and Eurasian plates has given rise to the great Himalaya. The long Himalayan mountain region keeps on generating a few great and several moderate earthquakes every century. This region has experienced six great earthquakes in a span of last 200 years or so, such as the earthquakes of 1803 Kumaon; 1833 Kathmandu; 1897 Shillong, M_w 8.1; 1905 Kangra, M_w 7.8; 1934 Bihar–Nepal, M_w 8.4; and 1950 Assam, M_w 8.7 (Bilham 2004; Kayal 2008). No great earthquake occurred in the Himalaya since 1950 (Khatttri 1999; Bilham 1995); however, recently, a major earthquake occurred in central Nepal region with M_w 7.9 named as the Nepal or Gorkha earthquake. The Himalayan geodynamics and the occurrence of great earthquakes are well reviewed by many researchers (e.g., Seeber and Armbruster 1981; Khatttri 1999; and Bilham and Gaur 2000). Some parts of the Himalayan Mountains have not experienced major and

✉ Himanshu Mittal
himanshumitt10@gmail.com

¹ Department of Geosciences, National Taiwan University, 10617 Taipei, Taiwan

² Department of Earthquake Engineering, Indian Institute of Technology, Roorkee 247667, India

³ National Center for Research on Earthquake Engineering, 10668 Taipei, Taiwan

⁴ Department of Earth Sciences, Indian Institute of Technology, Roorkee 247667, India

⁵ Department of Civil Engineering, Arni University, Kathgarh, Indora, Himachal Pradesh, India

great earthquakes in the past 100 years or so, though these have the potential to produce large earthquakes. Such segments are referred to as seismic gaps. Three main seismic gaps have been identified in the Himalaya (Fig. 1): the gap between the 1950 Assam and 1934 Bihar–Nepal earthquakes, known as the Assam gap; the gap between the 1905 Kangra and 1934 Bihar–Nepal earthquakes, known as the Central gap, and the Kashmir gap which lies west of the 1905 Kangra earthquake rupture (Seeber and Armbruster 1981; Khattri 1999). These gaps are considered as future possible zones of major earthquakes. A 750-km-long area of central seismic gap, lying between the eastern edge of the 1905 rupture zone and the western edge of the 1934 earthquake, remains unbroken (Bilham 1995). In 1803 and 1833, two large earthquakes occurred in the gap region with large magnitude values <8 , and hence, they are not regarded as gap-filling events (Khattri 1999; Bilham 1995). Khattri (1999) estimated the probability of occurrence of a great earthquake to be 0.59 in the central seismic gap in the next 100 years. A large earthquake in the central seismic gap is likely to cause great loss of life and severe damage to construction in Northern India. This accentuates the need for realistic assessment of ground motion from future earthquakes in the central seismic gap.

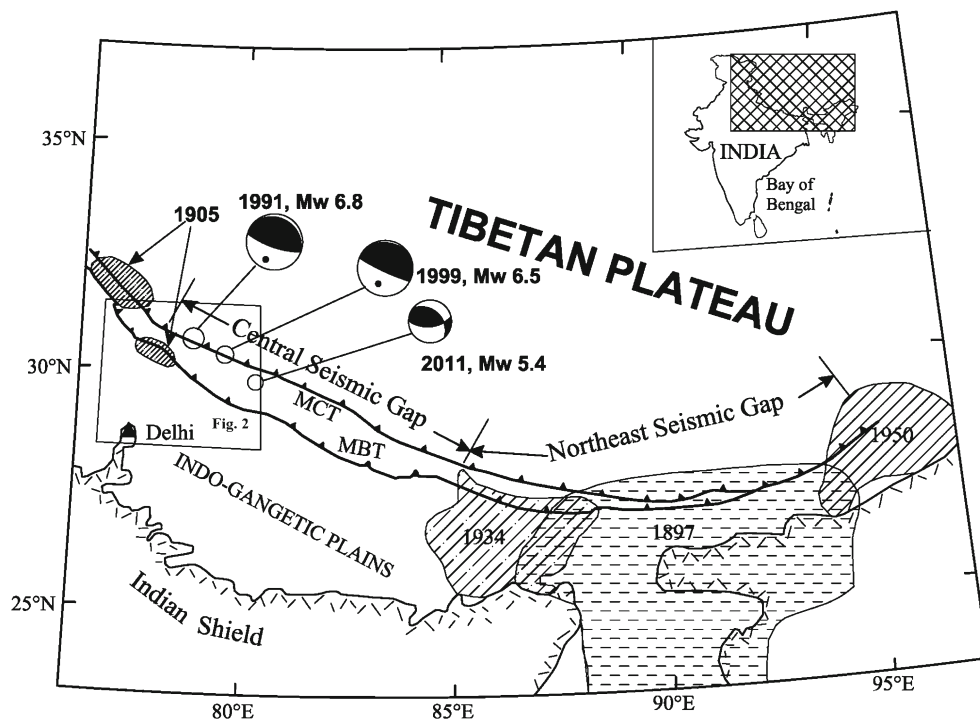
The most challenging issue in seismic hazard studies is to predict the ground motion at a given site due to future possible earthquakes. The ideal solution to this problem could be to use a wide database of recorded strong ground motion records and to group those accelerograms that have similar source, path and site effects. However, such data base will not be generally available for most sites. The alternative is empirical or

numerical simulation of strong ground motion, which has important applications in engineering seismology.

A number of procedures are used for simulating strong ground motions from future large earthquakes. These include stochastic technique, composite source technique, and empirical Green's function (EGF) techniques. Many researchers have used stochastic approaches to simulate strong ground motions in various parts of the world (Boore 1983; Toro and McGuire 1987; Singh et al. 2002; Mittal and Kumar 2015; Mittal et al. 2016). Another commonly used technique is the EGF technique. In the EGF technique, the recordings of small earthquakes adjacent to the target earthquake are used (Hartzell 1978; Irikura 1983; Ordaz et al. 1995; Sharma et al. 2013, 2016). Many works have been carried out in India using Ordaz et al. (1995) summation technique (e.g., Singh et al. 2002; Mittal et al. 2013b, 2015). One significant advantage of the EGF method comes from the fact that the wave propagation and the site effects are included in the recordings. We note, however, that the EGF method as applied in the present study assumes that the rupture can be approximated by a point source, an assumption that may be valid for $M_w \leq 7.5$ earthquakes but may not be rational for larger events (Singh et al. 2002).

The 1803 Kumaon earthquake occurred in the Kumaon–Garhwal Himalaya region between 77° and 81° E, west of Nepal, and caused severe damage and took a heavy toll of life in the densely populated region of the Gangetic plain between Delhi and Lucknow, over 300 km away to its east (Ambraseys and Jackson 2003). Over the past two decades, this region, which the focus of the present investigation, has witnessed several small to moderate-sized earthquakes, the most

Fig. 1 Tectonic map of the region (modified from Seeber and Armbruster 1981). Hatched areas denote intensity greater than or equal to VIII. The segment between the rupture areas of the 1905 and 1934 earthquakes is known as the central seismic gap, while the area between 1934 and 1950 earthquakes is called northeast seismic gap. Main central thrust (MCT); main boundary thrust (MBT) are shown. Locations and focal mechanisms of 1991 Uttarkashi, 1999 Chamoli, and Nepal border 2011 earthquakes are also shown



prominent being the August 19, 2008 (M_w 4.3), September 4, 2008 (M_w 5.1), October 3, 2009 (M_w 4.3), February 22, 2010 (M_w 4.7), May 1, 2010 (M_w 4.6), July 6, 2010 (M_w 5.1), April 4, 2011 (M_w 5.4), April 5, 2011 (M_w 5.0), and so on. Table 1 gives the complete detail about these earthquakes. In the present study, we take advantage of the EGF method proposed by Ordaz et al. (1995) to synthesize ground motions from future great earthquakes ($M_w = 7.5$) in the source region using recordings of the 2011 Nepal-India Border earthquake (M_w 5.4) as an element earthquake. This earthquake was recorded on strong motion accelerographs at 24 sites deployed by the Indian Institute of Technology (IIT), Roorkee. A great earthquake from the Himalayas may cause heavy loss of life as well as property in plain regions. Most of the areas in vicinity of the Himalayas have undergone extraordinary growth for various socioeconomic reasons. Taking into consideration the vulnerability of these areas, seismic hazard assessment from future earthquakes has become essential.

Seismotectonics

In the formation process of the Himalayas, it has created several fault systems to the south of the Indus–Tsangpo collision suture, marked by distinct lithotectonic boundaries. The Himalaya is divided into a number of sequences: Siwalik Group (sub-Himalaya), Lesser Himalayan Sequence (LHS), Greater Himalayan Crystallines (GHC), and Tethyan Himalayan Sequence (THS); each is bounded to the south

by a major north-dipping fault, such as the Main Frontal Thrust (MFT), the Main Boundary Thrust (MBT), and the Main Central Thrust (MCT). In the Kumaon–Garhwal Himalaya, the MCT is a zone bound by the Munsiri Thrust (MT) in the south and the Vaikrita Thrust (VT) in the north (Fig. 2). Geographically, the Kumaon and Garhwal regions lie in Uttarakhand state of India extending from the Sutlej River in the west to the Kali River in the east. Detailed geology of the region has been reviewed by Valdiya (1980); Yin (2006) and others. Besides these big Himalayan thrusts, several other faults and thrusts exist in the study area. Several faults and lineaments are transverse to the Himalayan trend. Important among these are Mahendragarh Dehradun Fault (MDF), Great Boundary Fault (GBF), and Moradabad fault (MF), which exists in the Delhi-Moradabad region.

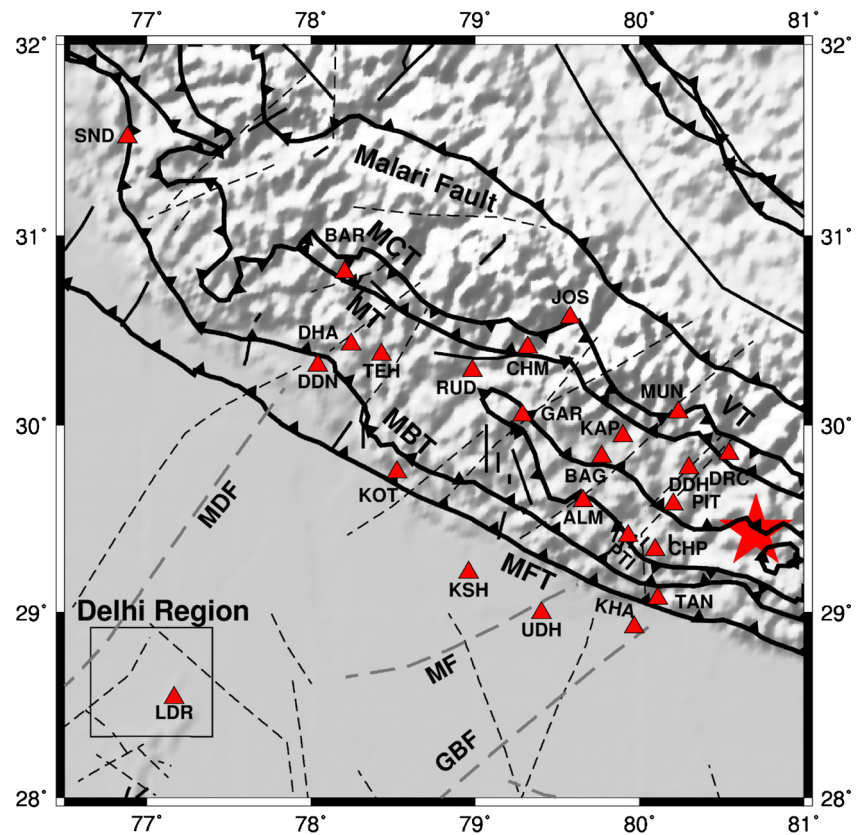
The distribution of seismicity throughout the Himalaya appears to be centered around in a 50-km-wide belt with moderate-sized events ($M_L < 6$) located beneath the lesser Himalaya between the MCT and the MBT (Seeber and Armbruster 1981; Khattri et al. 1989; Khattri 1999). Most of these events are located to the south of the MCT. Medium-sized earthquakes with well-determined fault plane solutions and focal depths determined by Ni and Barazangi (1984) define a simple planar zone situated at 10–20 km depth, with an apparent dip of 15° . This planar zone defines the detachment that separates the underthrusting Indian plate from the Lesser Himalaya crustal block and along which the great Himalayan earthquakes occurred during the past 90 years (Seeber and Armbruster 1981). Recent investigations in other segments

Table 1 Prominent earthquakes recorded in Kumaun Himalayas by strong motion network of IIT Roorkee

No.	Date dd/mm/year	Time hh:mm:ss.	Magnitude	Latitude °N	Longitude °E	No. of stations recording
1	19/08/2008	10:54:26	4.3	30.1	80.1	4
2	04/09/2008	12:53:21	5.1	30.1	80.4	7
3	27/08/2009	16:54:15	4.0	30.0	80.0	3
4	03/10/2009	05:20:54	4.3	30.0	79.9	3
5	11/01/2010	05:15:18	4.0	29.7	80.0	3
6	22/02/2010	17:23:43	4.7	30.0	80.1	6
7	01/05/2010	22:36:25	4.6	29.9	80.1	7
8	06/07/2010	19:08:20	5.1	29.8	80.4	2
9	04/04/2011	11:31:40	5.4	29.4	80.7	24
10	04/05/2011	20:57:15	5.0	30.2	80.4	1
11	26/02/2012	23:08:42	4.3	29.6	80.8	2
12	28/07/2012	05:48:06	4.5	29.7	80.7	2
13	23/08/2012	16:30:19	5.0	28.4	82.7	3
14	11/11/2012	18:39:19	5.0	29.2	81.5	3
15	02/01/2013	17:42:15	4.8	29.4	81.1	1
16	09/01/2013	07:44:20	5.0	29.7	81.7	4
17	29/01/2013	19:42:52	4.0	30.0	81.6	1

Only earthquakes with $M \geq 4.0$ are listed

Fig. 2 Seismotectonic setup of rectangle portion in Fig. 1. Various faults contributing to seismicity in the region, namely MBT, MCT, MFT, Vartica Thrust (VT), Muniari Thrust (MT), Malari Fault, Mahendragarh Dehradun Fault (MDF), Great Boundary Fault (GBF), and Moradabad fault (MF) are shown as *triangles*. All the strong motion stations recording the April 4, 2011 earthquake are shown. The epicenter of April 4, 2011 is shown as a *red star*



of the Himalaya show that apart from sporadic distributions, most of the seismicity in these segments is also clustered in a narrow zone, just south of the surface trace of the MCT (Kumar et al. 2009). However, earthquake focal depth estimates from the Nepal Himalaya (Monsalve et al. 2006; Liang et al. 2008) indicate the existence of two distinct seismogenic zones in the depth ranges of 0–25 km and 50–100 km, suggesting the near absence of earthquakes in the lower crust, of possibly lower strength (e.g., Chen and Molnar 1983).

Data

A strong motion network of 300 stations is being operated along the Himalayan arc by IIT Roorkee (Kumar et al. 2012). This network has recorded around 200 earthquakes in a span of 6 years since its installation (Mittal et al. 2012). The April 4, 2011 earthquake was recorded at 24 stations of this network. The closest instrument recording this earthquake was Dharchula (epicentral distance = 49 km), while the most distant was SunderNagar (epicentral distance = 434 km). The digital recordings of the mainshock, available to us for the analysis, are summarized in Table 2. Table 2 gives

characteristics of the recording system and the peak values of the recorded accelerations (A_{\max}) and the velocities (V_{\max}).

Synthesis of ground motion

We synthesize the expected ground motions using two methods. First method uses the recordings of April 4, 2011 earthquake as EGFs. The second method, called the point-source stochastic method (Hanks and McGuire 1981; Boore 1983), is based on the spectrum of the ground motion, which is described by a physically reasonable seismological source spectrum, modified by path and site effects. The advantage of the EGF method is that the wave propagation and the site effects are included in the recordings. However, as stated earlier, the EGF method applied here assumes that the rupture can be approximated by a point source, an assumption which may be valid for $M_w \leq 7.5$ earthquakes but may not be reasonable for larger events (Singh et al. 2002).

EGF method

A brief description of the method used in ground motion synthesis is given in the following section. The EGF method proposed by Ordaz et al. (1995) requires the specification of

Table 2 Peak acceleration and peak velocity at various stations during the April 4, 2011 earthquake

Epicentral distance (km)	Station	Station code	$A_{max}(cm/s^2)$			$V_{max}(cm/s)$		
			NS	EW	Vert	NS	EW	Vert
49	Dharchula	DRC	131.63	131.81	56.22	8.26	6.89	1.42
51	Pithoragarh	PIT	60.30	60.49	37.07	1.17	1.62	0.85
55	Didihat	DDH	18.82	16.35	12.68	1.11	0.84	0.52
60	Champawat	CHP	17.10	31.55	10.64	0.65	0.90	0.40
70	Tanakpur	TAN	11.19	12.41	7.80	0.59	0.51	0.31
75	Patti	PTI	9.11	4.71	3.93	0.47	0.26	0.23
84	Munsiari	MUN	25.09	19.15	12.75	0.83	0.80	0.37
92	Khatima	KHA	20.83	25.81	8.32	1.30	1.75	0.36
101	Bageshwar	BAG	9.86	10.86	4.30	0.82	0.44	0.23
103	Almora	ALM	9.66	10.66	-7.59	0.52	0.63	0.31
136	U. S. Nagar	UDH	8.25	10.98	5.57	0.62	0.94	0.27
154	Garsain	GAR	19.24	20.36	12.85	1.15	1.10	0.59
167	Joshimath	JOS	10.28	10.91	5.60	0.68	0.52	0.42
171	Kashipur	KSH	10.25	8.82	7.22	0.59	0.49	0.28
173	Chamoli	CHM	17.50	11.12	8.76	1.69	1.21	0.70
192	Rudraprayag	RUD	6.34	7.74	3.65	0.34	0.37	0.20
214	Kotdwar	KOT	4.10	6.41	4.12	0.32	0.30	0.14
243	Tehri	TEH	5.92	6.48	4.09	0.30	0.39	0.23
262	Dhanaulti	DHA	7.21	7.45	2.14	0.49	0.63	0.13
275	Dehradun	DDN	3.29	3.17	1.54	0.27	0.23	0.08
276	Roorkee	ROO	4.62	3.52	1.56	0.32	0.33	0.11
285	Barkot	BAR	6.10	7.82	2.51	0.28	0.43	0.12
352	Lodhi Road	LDR	1.85	1.79	1.28	0.17	0.17	0.06
434	Sundernagar	SND	2.96	2.32	1.10	0.22	0.17	0.08

the seismic moment, M_0 , and the stress drop, $\Delta\sigma$, of both the EGF and the target event. The point-source stochastic method requires the specification of the stress drop of the target event and knowledge of the path and the site effects. In the following, we take M_0 of the present earthquake as 1.56×10^{24} dyne cm, which is the scalar seismic moment reported in the Harvard CMT catalog. The effective duration of the ground motion is taken as $T_s + T_d = 1/f_c + 0.05R$, where T_s and T_d are the source duration and path duration, respectively (Herrmann 1985). Then, we use network recordings of the April 4, 2011 earthquake in order to estimate parameters needed in the EGF method.

Source spectrum

In order to estimate the stress drop, $\Delta\sigma$, of the April 4, 2011 earthquake and the quality factor, Q , between the source region and Delhi, the spectra of the recordings at Delhi are analyzed. This analysis is given by Eqs. (1–5). The source displacement and acceleration spectra of the two earthquakes, $M_0(f)$ and $f^2 M_0(f)$, are estimated from the analysis of the S-wave

recorded at hard sites (ALM, BAG, PTI, MUN) from the recording of the India–Nepal border earthquake of April 4, 2011.

The Fourier acceleration spectral amplitude of the intense part of the ground motion at a distance R from the source, $A(f, R)$, can be written as follows:

$$A(f, R) = \frac{CS(f)e^{-\pi R/\beta Q(f)}}{G(R)} \tag{1}$$

$$C = \frac{R_{\theta\phi} FP(2\pi)^2}{(4\pi\rho\beta^3)} \tag{2}$$

$$S(f) = f^2 \dot{M}_0(f) \tag{3}$$

$$S(f) = \frac{f^2 f_c^2 M_0}{(f^2 + f_c^2)} \tag{4}$$

$$f_c = 4.9 \times 10^6 \times \beta \left(\frac{\Delta\sigma}{M_0} \right)^{\frac{1}{3}} \tag{5}$$

$$\log A(f, R) + \log G(R) - \log C = \log S(f) - 1.36fR/\beta Q(f) \tag{6}$$

In the equations above, $M_0(f)$ is the moment rate spectrum so that $M_0(f) \rightarrow M_0$ as $f \rightarrow 0$, R is hypocentral distance, C is

given by Eq. (2), β is shear wave velocity (3.7 km/s), $Q(f)$ is quality factor which includes both anelastic absorption and scattering, ρ is focal region density (2.85 gm/cm^3), $R_{\theta\phi}$ is average radiation pattern (0.55), F is free surface amplification (2.0), P takes into account the partitioning of energy in the two horizontal components ($1/\sqrt{2}$), and f_c is corner frequency. $G(R)$ in Eq. (1) is the geometrical spreading term, which is taken as $1/R$ for $R \leq 100 \text{ km}$ and $(100R)^{-1/2}$ for $R > 100 \text{ km}$ (Singh et al. 1999).

Equation (1) was simplified to Eq. (6). Finally, Eq. (6) was solved in the least square by putting value of different unknowns and constants to obtain the value of $\log(f^2 M_0(f))$. The source spectra is shown in Fig. 3. Figure 3a shows source displacement spectrum (continuous curve), $M_0(f)$ and source acceleration spectrum (dashed curve), $f^2 M_0(f)$ determined from the hard rock sites data using Eqs. (1–5). The spectrum is corrected using $Q(f) = 508f^{0.48}$, a relationship found by Singh et al. (1999) for the Indian shield region. The hard-site spectra is interpreted by an ω^2 -source model to obtain an estimation of the seismic moment (M_0) and corner frequency (f_c).

For an ω^2 source model, the source acceleration spectrum is flat at frequencies greater than the corner frequency, f_c . In Fig. 3a, this is the case for $f > 1 \text{ Hz}$. Both the low and high-frequency levels of the spectrum are well fit by the ω^2 -source model with $M_0 = 1.56 \times 10^{24} \text{ dyne cm}$ and $f_c = 1.19 \text{ Hz}$ (corresponding to a stress drop, $\Delta\sigma$, of 362 bars, Eq. 5). Figure 3b shows source spectrum at some of the soft soil sites namely Roorkee, Delhi, and others, portraying the presence of amplification in recordings, where it deviates from the theoretical source spectrum. The local site condition plays an important

role in controlling amplification of the earthquake ground motion and associated damages to the structures.

Site effects

The estimation of ground motion from future earthquakes heavily relies on recorded ground motion as well as site effects of the stations, where it is recorded. Several techniques are available to estimate site effects due to local site conditions (Borcherdt 1970; Nakamura 1989; Lermo and Chavez-Garcia 1993). The most commonly used technique for estimation of site effects is to divide the Fourier spectrum of the site by the Fourier spectrum obtained at a nearby reference site, which is preferably on the bedrock, which gives transfer function of the site. Although this approach assumes linear behavior of soil (i.e., transfer function will be same irrespective of level of shaking) which is not correct but this assumption will have negligible effect on hard rock site and will have only marginal effect on other sites. This technique invented by Borcherdt (1970) is widely used in various geological environments in India (Singh et al. 2002; Mittal et al. 2013a, c). However, in many cases, it becomes difficult to choose a reference site (Steidl et al. 1996). In addition, outcrops of bedrock sites are usually weathered, and the resulting superficial velocity gradient is capable of influencing the “reference” ground motion. Another equivalent technique to estimate site effect is the horizontal-to-vertical (H/V) spectral ratio method. This technique was originally proposed for microtremors (Nakamura 1989) but later successfully applied in strong-motion studies also (e.g., Lermo and Chavez-Garcia, 1993). This technique

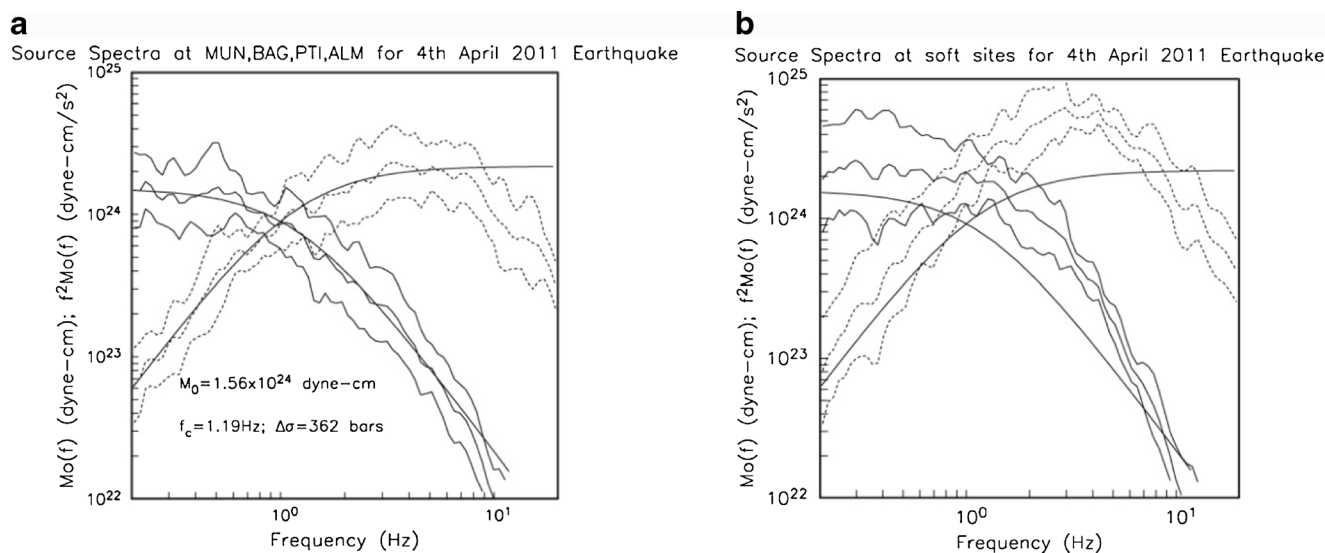


Fig. 3 Source displacement (*continuous curves*) and acceleration spectra (*dashed curves*), $M_0(f)$ and $f^2 M_0(f)$ of the April 4, 2011 earthquake. Median and \pm one standard deviation curves are shown. **a** Data from MUN, ALM, BAG, and PTI four hard site. The spectra are reasonably

well fit by an ω^2 -source model with $M_0 = 1.56 \times 10^{24} \text{ dyne cm}$ and a corner frequency of 1.19 Hz. **b** Source spectrum using the data from soft soil sites showing the presence of site effects

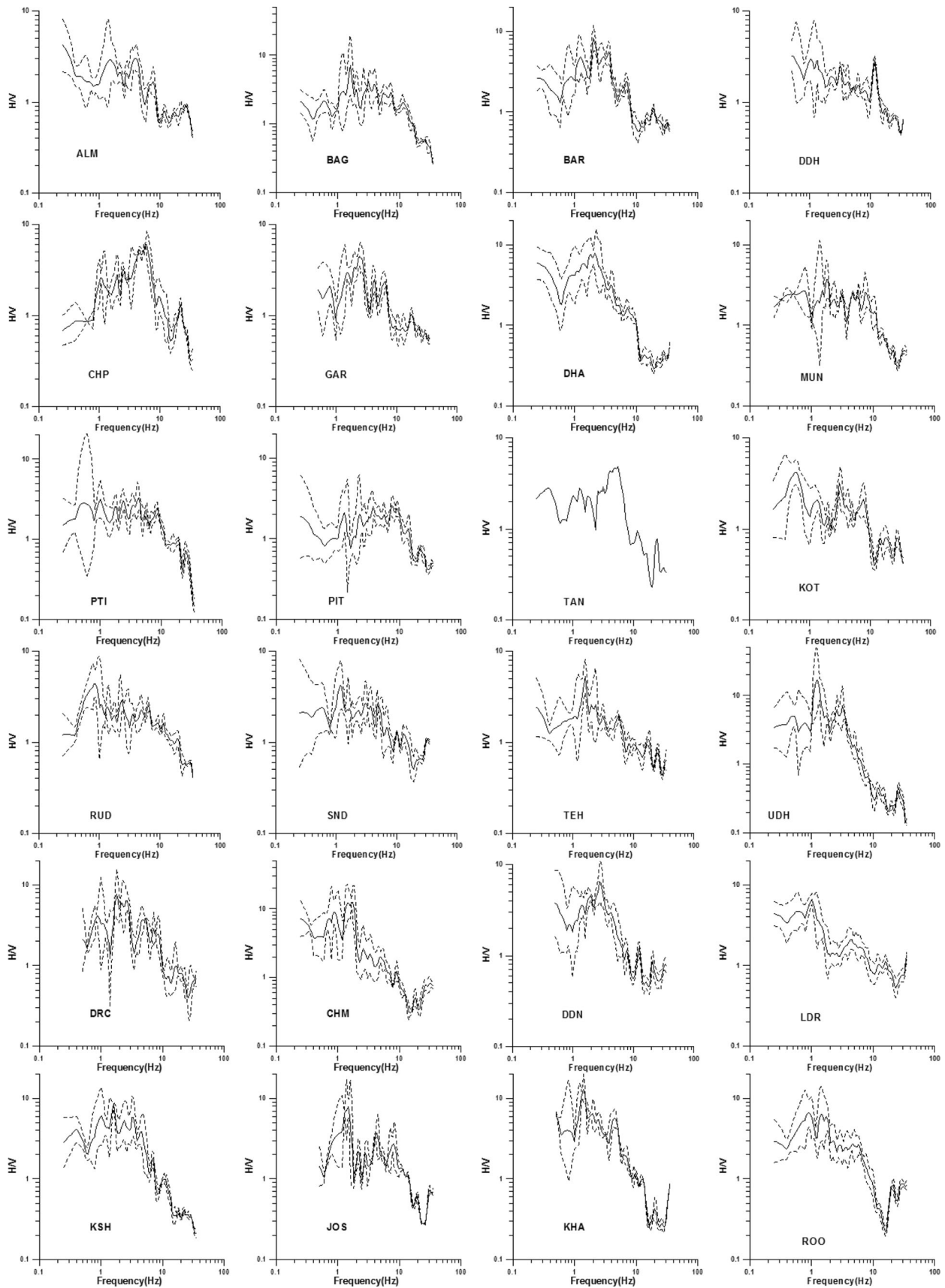


Fig. 4 Average H/V ratio at various stations used in the present work. The *dashed curves* in each figure represent \pm standard deviation

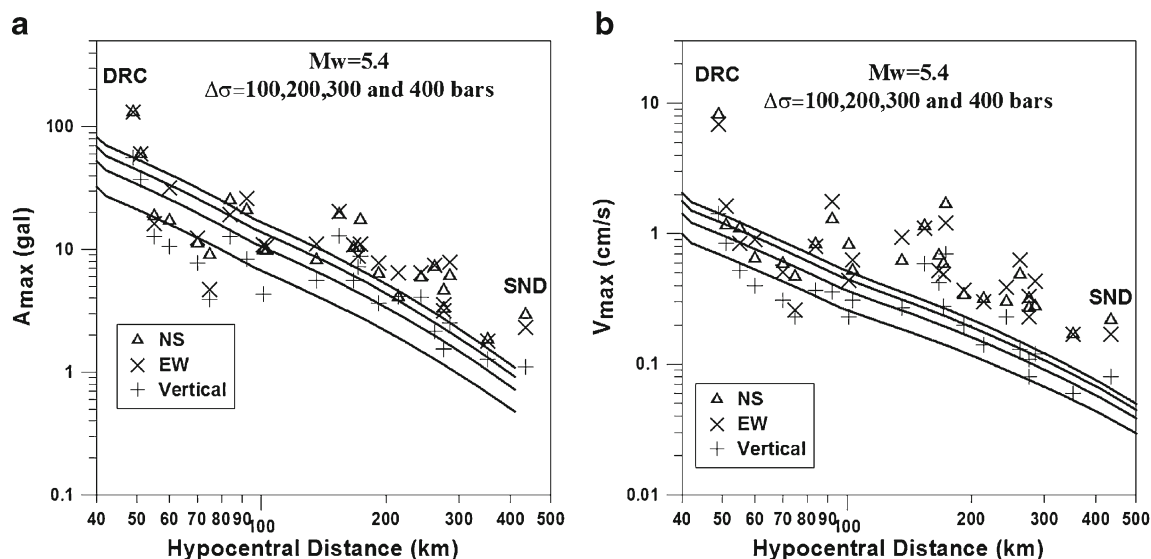


Fig. 5 Observed peak ground motion (different symbols for different components) versus hypocentral distance R during the April 4, 2011 earthquake. Continuous curves show estimated values at hard site for four values of stress drops (100, 200, 300, and 400 bars), based on the

point-source stochastic model. **a** A_{max} ; **b** V_{max} . DRC refers to nearest site of Dharchula while SND is used for SunderNagar site at a distance of 434 km

consists in estimating site effects by dividing the horizontal component of the shear-wave spectrum by the vertical component at the site. In the present study, the H/V spectral ratios are estimated using the S-wave portions of recording of April 4, 2011 and some other earthquakes at various stations.

The site amplification functions have been estimated using H/V technique in order to incorporate the site effects to the simulated accelerograms at bed rock level. To compute the H/V spectral ratio, the acceleration time series of each recording station is windowed for a time length of 15 s. The small window length may influence the estimation for the lower frequencies (less than 0.4 Hz). However, final results may not get affected as the earthquake strong ground motions are dominated by the high-frequency energy. At each site, two to three earthquakes are carefully selected for the site effect analysis depending on the signal-to-noise ratio. The time window was selected from the shear-wave arrival time, and a 5 % cosine taper was applied. The windowed time series is transformed into the frequency domain using a fast Fourier transform algorithm. The obtained Fourier spectra between 0.25 and 35 Hz are smoothed using the windowing function of Konno and Ohmachi (1998) with smoothing constant = 40. Figure 4 shows average H/V ratio at all stations.

The results obtained from H/V method are affected by local and subsurface factors which influence the vertical component of ground motion. Some factors are (1) role of compressional deformation (P wave) to vertical component at frequencies higher than 8–10 Hz (Beresnev et al. 2002), (2) amplitude increase in vertical components due to non-linear effects (Loukachev et al. 2002), and (3) P wave conversion from the SV waves at the boundaries of the layers above the base rock (Tohdo et al. 1995). All these effects can be reduced by

using data only from rock stations (Sokolov et al. 2007). According to the seismotectonics atlas map of India, stations namely Almora, Bageshwar, Chamoli, Champawat, Tehri, Barkot, Dharchula, Garsain, Pithoragarh, Munsiari, Patti, Rudraprayag, Didihat, Sundernagar, and Tehri are considered to be hard rock sites. The shear wave velocity at these sites ranges from 700 to 1620 m/s (Mittal et al. 2012). As evident from Fig. 4, fundamental frequency at all these sites ranges between 3 and 6 Hz. However, at few stations, the H/V ratios are large in certain frequency bands. The fundamental phenomenon responsible for it may be soil-building interaction because these stations are not installed in free field. It may also be attributed to the local subsurface influencing the vertical component. Such sites require independent site response analysis using some other technique.

At the rest of the sites namely, Kashipur, Khatima, Roorkee, Delhi, and Dehradun, the fundamental frequency is observed below 2 Hz. The amplification at these sites ranges between 5 and 10.

Point source stochastic method

If only peak ground motion parameters are desired, then the generation of the seismograms is not needed; the Fourier spectrum along with an estimation of duration (T_R) of the intense part of the ground motion and application of results from random vibration theory (RVT) solve the problem.

This method was first proposed by Hanks and McGuire (1981) and later extended by Boore (1983). Hanks and McGuire (1981) related root mean square (rms) acceleration to ω^2 -source spectrum modified by attenuation, through Parseval's theorem. In this method, the spectrum of the ground

Table 3 Comparison of observed and computed peak values at different sites

Station	Observed $A_{max}(cm/s^2)$		Synthesized $A_{max}(cm/s^2)$	Observed $V_{max}(cm/s)$		Synthesized $V_{max}(cm/s)$
	NS	EW		NS	EW	
Dharchula	131.63	131.81	103.51	8.26	6.89	5.94
Pithoragarh	60.30	60.49	60.32	1.17	1.62	1.90
Didihat	18.82	16.35	34.30	1.11	0.84	1.55
Champawat	17.10	31.55	43.10	0.65	0.90	0.71
Tanakpur	11.19	12.41	25.17	0.59	0.51	0.89
Patti	9.11	4.71	19.30	0.47	0.26	0.75
Munsiari	25.09	19.15	23.71	0.83	0.80	1.07
Khatima	20.83	25.81	26.71	1.30	1.75	1.93
Bageshwar	9.86	10.86	18.31	0.82	0.44	0.91
Almora	9.66	10.66	12.34	0.52	0.63	0.65
U. S. Nagar	8.25	10.98	15.28	0.62	0.94	1.39
Garsain	19.24	20.36	12.90	1.15	1.10	0.76
Joshimath	10.28	10.91	8.58	0.68	0.52	0.59
Kashipur	10.25	8.82	10.33	0.59	0.49	0.77
Chamoli	17.50	11.12	10.86	1.69	1.21	1.05
Rudraprayag	6.34	7.74	6.35	0.34	0.37	0.45
Kotdwar	4.10	6.41	4.07	0.32	0.30	0.28
Tehri	5.92	6.48	3.51	0.30	0.39	0.25
Dhanaulti	7.21	7.45	7.11	0.49	0.63	0.57
Dehradun	3.29	3.17	4.43	0.27	0.23	0.32
Roorkee	4.62	3.52	4.30	0.32	0.33	0.47
Barkot	6.10	7.82	5.95	0.28	0.43	0.41
Lodhi Road	1.85	1.79	2.04	0.17	0.17	0.24
Sundernagar	2.96	2.32	2.02	0.22	0.17	0.19

The comparison looks in rough agreement

motion is related to the root mean square (rms) amplitude in the time domain through Parseval’s theorem (Cartwright and Longuet-Higgins 1956). RVT approach is an alternative to conventional site response analysis, which has been proposed in the engineering seismology literature. RVT-based site response is an extension of stochastic ground motion simulation procedures developed by seismologists to predict peak ground motion parameters (e.g., peak ground acceleration) as a function of earthquake magnitude and site-to-source distance. Due to its stochastic nature, RVT analysis can provide an estimate of the site response without the need to choose any input seismograms for analysis. Therefore, RVT is a potentially powerful tool for site response analysis that can provide fast and accurate estimates of the surface ground motion at a site (e.g., Boore 1983). Boore (1983) extended these results to predict V_{max} and response spectra by generating time series of filtered and windowed Gaussian noise whose amplitude spectrum approximated the acceleration spectrum. Here, we briefly summarize some relevant aspects of the method.

For an ω^2 -source model, the source spectrum of an earthquake is completely specified by its seismic moment and the stress drop (Eqs. 1–5). To simulate the observed spectra at a site, the right-hand side of Eq. (1) needs to be multiplied by a high-cut filter. Following Boore (1986), a Butterworth filter

given by $\left[1 + \left(f/f_m\right)^8\right]^{-\frac{1}{2}}$ is chosen (Singh et al. 1999). In our calculations, we have set f_m to 35 Hz. Figure 5 shows expected A_{max} and V_{max} at hard rock for $Q(f)=508f^{0.48}$, and $\Delta\sigma = 100, 200, 300,$ and 400 bars. Figure 5a, b shows plots of A_{max} and V_{max} versus hypocentral distance R , respectively. As seen from Fig. 5a, computed PGA at some of the sites (hard rock sites) matches well with the observed one. However, at some sites, the computed PGA lies below the observed one. We feature this large scattering seen in the observed peak values most probably due to variable local site effects. Table 3 shows the comparison of observed PGA and PGVs with computed one (using point source approximation technique) after introduction of site effects. From Table 3 it is obvious that peak values at most of the sites are in rough

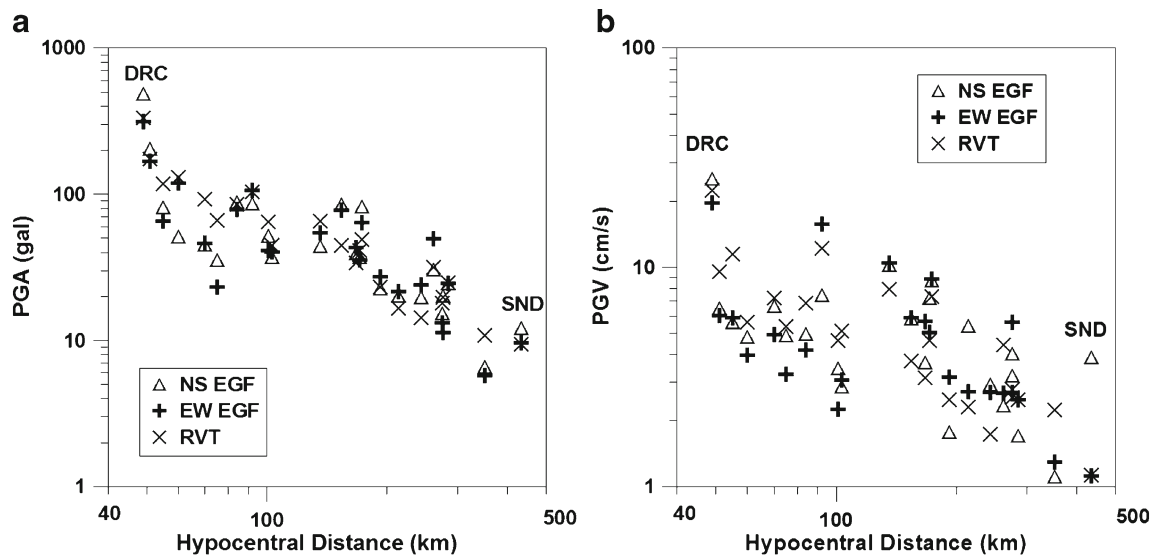


Fig. 6 Comparison of peak values for M_w 6.5 estimated from EGF (different symbols for different components) and RVT technique. **a** PGA; **b** PGV. A good agreement is found in both PGA and PGV values by two techniques

agreement. This agreement is well explained by taking $\Delta\sigma = 200$ bars. This gives us confidence that the parameters chosen in the simulations are practical.

Results and discussion

We estimated the M_w 7.0 and 7.5 scenario ground motions at various sites using the aforesaid two methods. M_0 of the present earthquake is taken as 1.56×10^{24} dyne cm while $\Delta\sigma$ is fixed to be 362 bars. The estimated values of A_{max} and V_{max}

for all components as function of M_w are summarized in Figs. 6, 7, 8 and 9. For M_w 7.0, the expected A_{max} and V_{max} on horizontal components at different sites range between 11 and 912 gal and 5 and 52 cm/s, respectively. The corresponding values for the Z component range between 8 and 228 gal and 3 and 14 cm/s, respectively. Similarly for M_w 7.5, the expected A_{max} and V_{max} on horizontal components at different sites range between 25 and 1281 gal and 25 and 102 cm/s, respectively. The corresponding values for the Z component range between 14 and 474 gal and 15 and 70 cm/s, respectively. It is evident that the estimated peak values from two

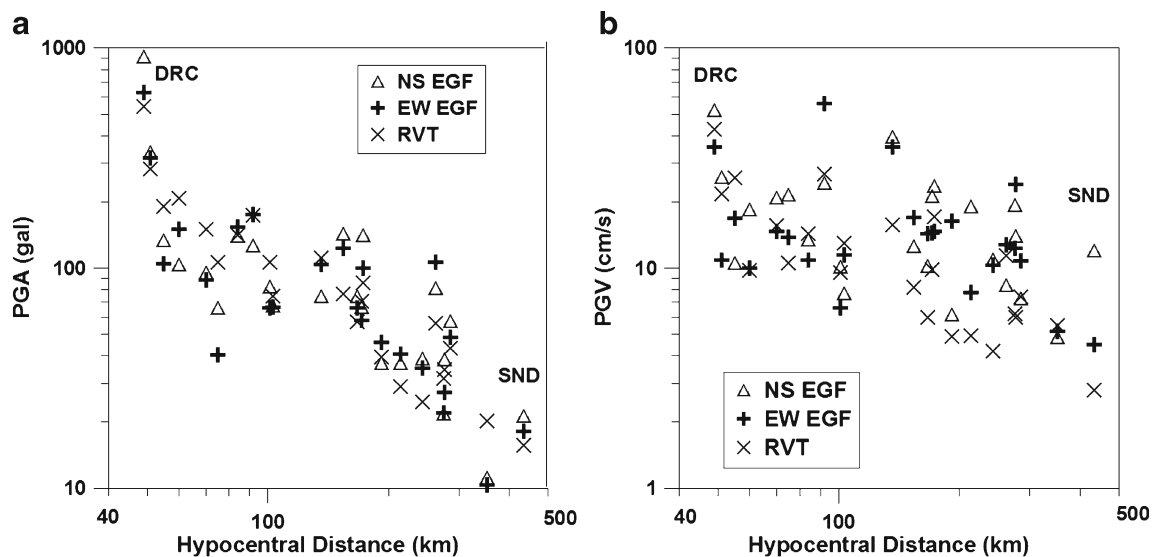


Fig. 7 Comparison of peak values for M_w 7.0 estimated from EGF (different symbols for different components) and RVT technique. **a** PGA; **b** PGV. A good agreement is found in both PGA and PGV values by two techniques

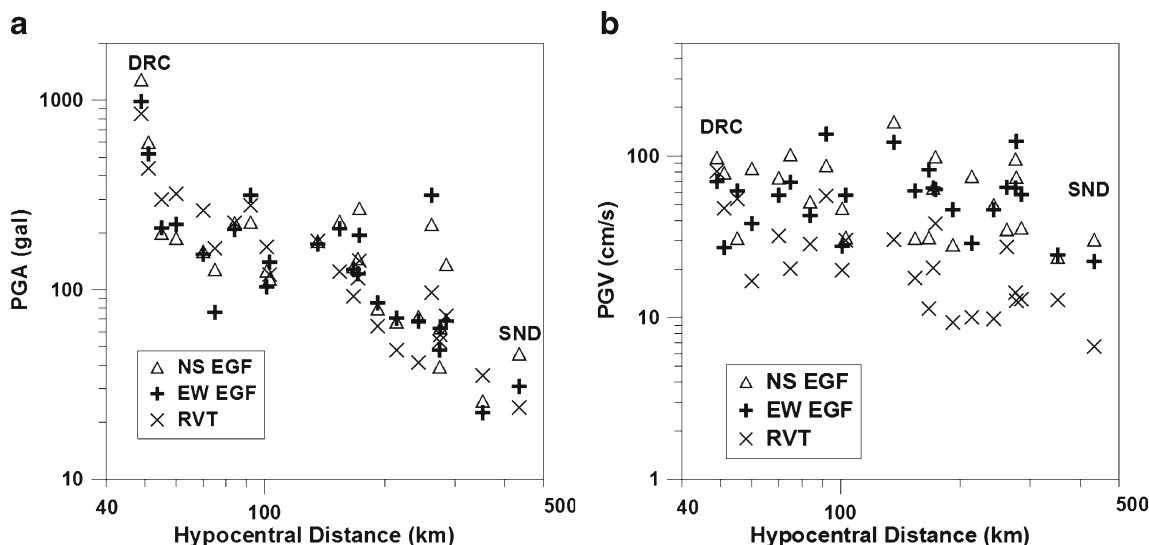


Fig. 8 Comparison of peak values for M_w 7.5 estimated from EGF (different symbols for different components) and RVT technique. **a** PGA; **b** PGV. A good agreement is found in PGA values by two techniques. Scattering is observed in PGV values by two techniques

techniques are in good agreement with each other for $M_w \leq 7.5$. For M_w 8.0, a large scattering is observed in peak values (especially in PGV), where finiteness of source comes in play.

Figure 10 shows the synthesized accelerograms (NS component) from one of the simulations for different magnitude earthquakes. However, these results regarding PGAs, PGVs, and synthesized traces for postulated earthquakes may be valid only if the hypothetical earthquake would occur at the same source as that of the April 4, 2011 earthquake.

Response spectra

From the synthetic seismograms, we estimate the horizontal response spectra, S_a , with 5 % damping at different sites during various postulated earthquakes. The seismic zonation map

for India (BIS IS 1893, 2002) shows that out of 24 sites, Dharchula, Pithoragarh, Didihat, Munsiri, Patti, Bageshwar, Almora, Chamoli, Rudraprayag, Joshimath, SunderNagar, and Garsain fall in zone V (on a scale of II to V), while other sites fall in zone IV. Estimated S_a for different magnitude scenario earthquakes at all sites known to fall in seismic zone V are grouped together and compared with IS 1893-2002 spectra for hard rock sites with a zero period acceleration (ZPA) of 0.36 g (type I). Also estimated S_a for different magnitude scenario earthquakes at all sites known to have stiff soil in zone IV are grouped together and compared with IS 1893-2002 spectra for stiff soil with a ZPA of 0.24 g (type I). IS 1893-2002 is the Indian standard code for earthquake resistant design of structures, and this code provides response spectra with unity ZPA for three types of soil.

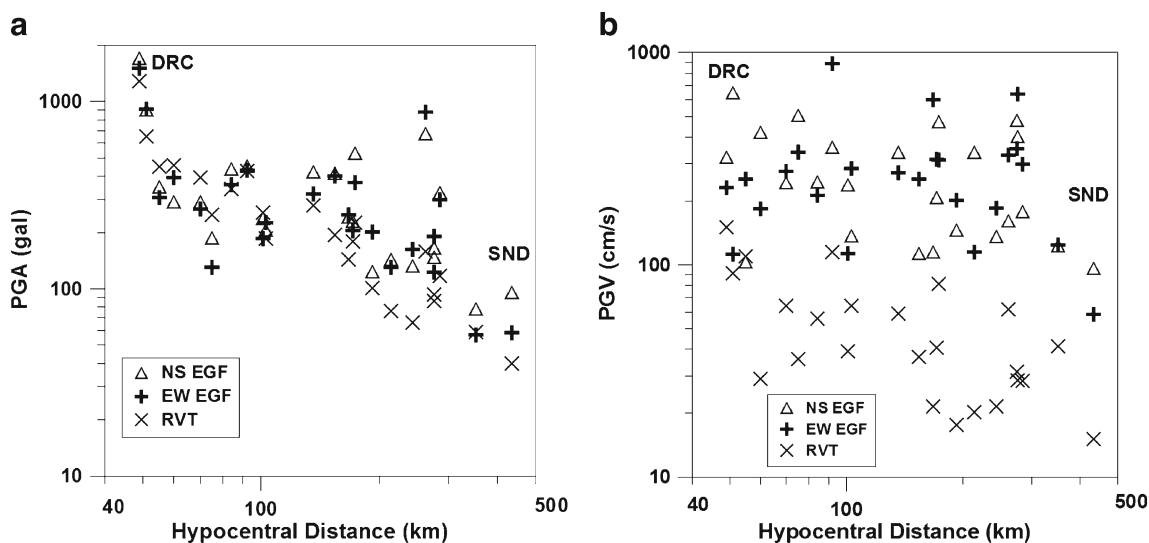


Fig. 9 Comparison of peak values for M_w 8.0 estimated from EGF (different symbols for different components) and RVT technique. **a** PGA; **b** PGV. Large scattering is observed in both PGA and PGV values by two techniques

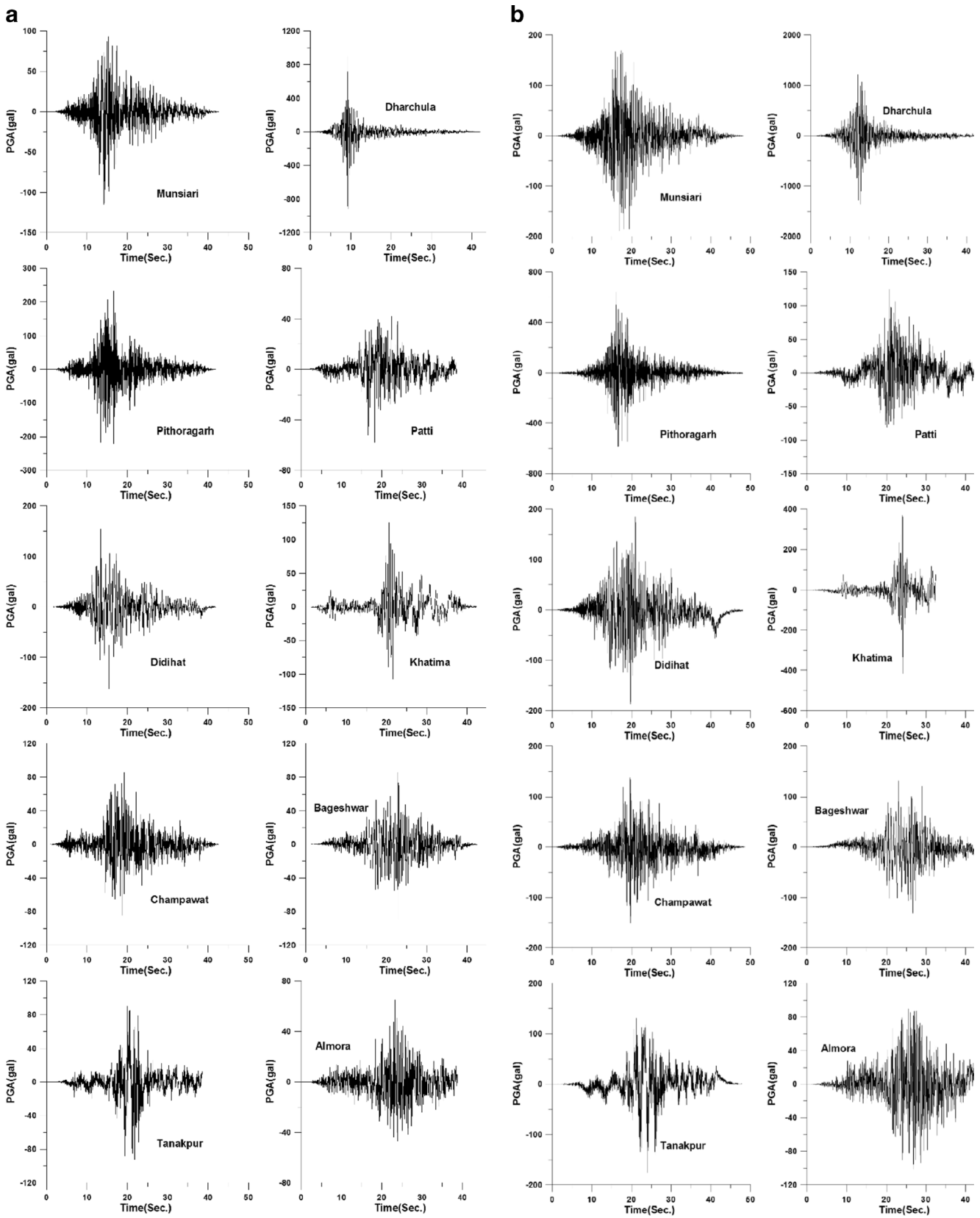


Fig. 10 Synthesized acceleration seismograms at some of the sites for different scenario earthquakes. **a** 7.0 magnitude, **b** 7.5 magnitude

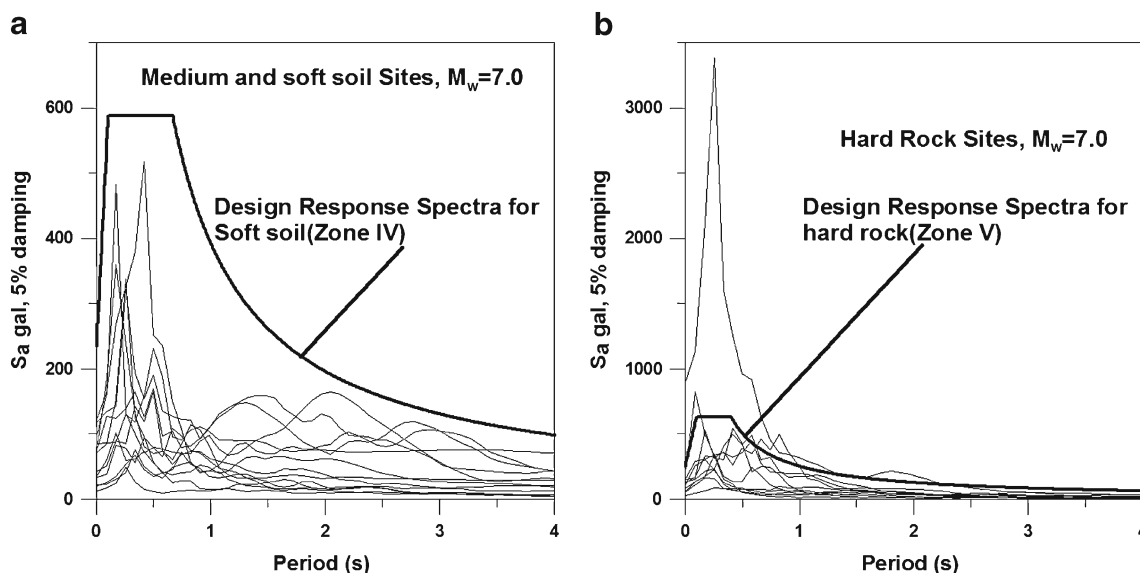


Fig. 11 Comparison of response spectra from $M_w = 7.0$ with design response spectra for zone IV and V of the Indian seismic zoning map (IS1893: 2002) valid in India. **a** Sites falling in zone IV. **b** Sites falling in zone V

Figure 11a shows that the zone IV response spectrum is deficient for $M_w 7.0$, while zone V response spectrum is exceeded at several frequencies for same (Fig. 11b). For $M_w 7.5$, the zone IV response spectrum is conservative (except at some frequencies), while zone V response spectrum is exceeded at many sites as evident from Fig. 12b.

Conclusions

Uttarakhand is a state of India, which is located in the seismically active Himalayan region and in the proximity of plate boundaries. Uttarakhand lies in the region between epicenters

of two huge earthquakes namely Kangra (1905) and Bihar Nepal earthquakes (1934). This seismic gap (Khattari 1987) has not experienced a major earthquake during a time interval when most other segments of the gap have ruptured. In view of this, estimation of seismic hazard in this area is an urgent need.

In this work, an attempt has been made to understand and quantify seismic hazard of different parts of Uttarakhand by synthesizing seismograms for different magnitude earthquakes using strong motion records of the April 4, 2011 earthquake. It is observed from synthesized seismograms that sites located near the epicenter, like Dharchula, may expect accelerations in excess of 1 g for earthquake of magnitude 7.5 or

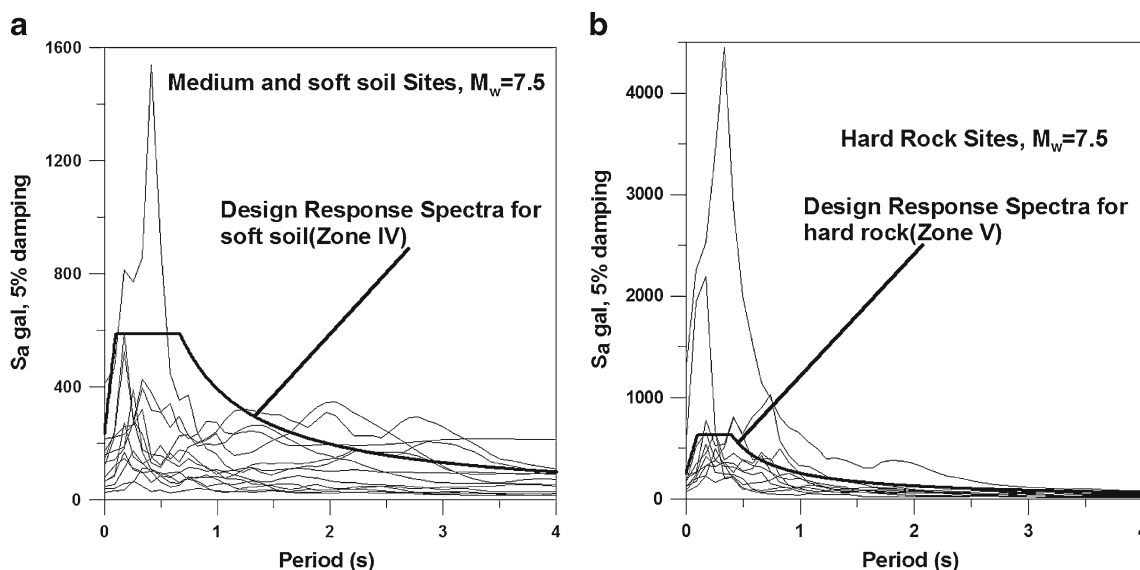


Fig. 12 Comparison of response spectra from $M_w = 7.5$ with design response spectra for zone IV and V of the Indian seismic zoning map (IS1893: 2002) valid in India. **a** Sites falling in zone IV. **b** Sites falling in zone V

more. Our computation of ground motion for scenario M_w 7.0, and 7.5 earthquakes show that for M_w 7.0, the expected A_{\max} and V_{\max} on horizontal components at different sites range between 11 and 912 gal and 5 and 52 cm/s, respectively. The corresponding values for the Z component range between 8 and 228 gal and 3 and 14 cm/s, respectively. Similarly, for M_w 7.5, the expected A_{\max} and V_{\max} on horizontal components at different sites range between 25 and 1281 gal and 25 and 102 cm/s, respectively. The corresponding values for the Z component range between 14 and 474 gal and 15 and 70 cm/s, respectively. Zone IV response spectrum for 5 % damping, valid for zone IV sites is generally conservative except at some periods of 3–4 sites for M_w 7.0, while zone V response spectrum is exceeded at several frequencies, particularly for Dharchula for same magnitude earthquake. For M_w 7.5, zone IV response spectrum is conservative (except at some frequencies, particularly for Khatima, Tanakpur, and Udham Singh Nagar sites), while zone V response spectrum is exceeded at many sites namely Dharchula, Pithoragarh, Chamoli, and Garsain.

The conclusions above are based on limited data and, hence, are necessarily preliminary. These results will be valid only if an earthquake occurs at same epicenter as that of April 4, 2011. The synthesis is being carried out using the EGF technique, which is point source approximation. In future, other techniques must be used to validate the results of present work. Detailed studies need to be undertaken for soil investigation at all the sites. This will help in determining the local site effects more accurately for assessment of amplification of ground motion.

Acknowledgments The authors are profusely thankful to Prof. S.K. Singh, Instituto de Geofísica, Universidad, Nacional Autónoma de México (UNAM) for providing the codes of his program. The authors are thankful to Ministry of Earth Science (MoES), Government of India and Ministry of Science and Technology, Republic of China, for funding projects under which this research and revision of manuscript was carried out. We are also very thankful to editor-in-chief, Abdullah M. Al-Amri for his valuable revision, which helped us to clarify and improve this paper. Comments from an anonymous reviewer helped in improving the manuscript. The strong motion data from IITR network is freely available from website www.pesmos.in (last accessed January 2015) to the registered users. We acknowledge the IITR network for the same. The GMT software from Wessel and Smith (1998) was used in plotting part of the figures and is gratefully acknowledged.

References

- Ambraseys N, Jackson D (2003) A note on early earthquakes in Northern India and Southern Tibet. *Curr Sci* 84(4):570–582
- Beresnev IA, Nightengale AM, Walter J, Silva WJ (2002) Properties of vertical ground motions. *Bull Seismol Soc Am* 92:3152–3164
- Bilham R (1995) Location and magnitude of the Nepal earthquake and its relation to the rupture zones of the contiguous great Himalayan earthquakes. *Curr Sci* 69:101–128
- Bilham R (2004) Earthquakes in India and the Himalaya: tectonics, geodesy and history. *Ann Geophys* 47(2/3):839–858
- Bilham R, Gaur VK (2000) The geodetic contribution to Indian seismotectonics. *Curr Sci* 79:1259–1269
- BIS IS 1893 (2002) (Part 1). Indian standard criteria for earthquake resistant design of structures, part 1—general provisions and buildings. Bureau of Indian Standards, New Delhi, p. 39
- Boore DM (1983) Stochastic simulation of high-frequency ground motions based on seismological models of the radiated spectra. *Bull Seism Soc Am* 73:1865–1884
- Boore DM (1986) The effect of finite bandwidth on seismic scaling relationships, in earthquake source mechanics, S. Das, J. Boatwright, and C. Scholz (editors). *Am Geophysical* 37:275–283
- Borcherdt RD (1970) Effects of local geology on ground motion near San Francisco Bay. *Bull Seism Soc Am* 60:29–61
- Cartwright DE, Longuet-Higgins MS (1956) The statistical distribution of the maxima of a random function. *Proc Roy Soc London, Ser A* 237:212–232
- Chen W, Molnar P (1983) Focal depths of intracontinental and intraplate earthquakes and their implications for the thermal and mechanical properties of the lithosphere. *J Geophys Res* 88:4183–4214
- Hanks TC, Mcguire RK (1981) The character of high-frequency strong ground motion. *Bull Seism Soc Am* 71:2071–2095
- Hartzell S (1978) Earthquake aftershock as Green's functions. *Geophys Res Lett* 5:1–4
- Herrmann RB (1985) An extension of random vibration theory estimates of strong ground motion at large distances. *Bull Seism Soc Am* 75:1447–1453
- Irikura K (1983) Semi-empirical estimation of strong ground motions during large earthquakes. *Bulletin of Disaster Prev Res Institute, Kyoto Univ* 32:63–104
- Kayal JR (2008) Microearthquake seismology and seismotectonics of South Asia. Springer, 504p
- Khattri KN (1987) Great earthquakes, seismicity gaps and potential for earthquake disaster along the Himalaya plate boundary. *Tectonophysics* 138:79–92
- Khattri KN (1999) An evaluation of earthquakes hazard and risk in Northern India. *Himal Geol* 20:1–46
- Khattri KN, Chander R, Gaur VK, Sarkar I, Kumar S (1989) New seismological results on the tectonics of the Garhwal Himalaya. *Proc Indian Acad Sci (Earth Planet Sci.)* 98:91–109
- Konno K, Ohmachi T (1998) Ground-motion characteristics estimated from spectral ratio between horizontal and vertical components of microtremor. *Bull Seism Soc Am* 88(1):228–241
- Kumar A, Mittal H, Sachdeva R, Kumar A (2012) Indian strong motion instrumentation network. *Seismol Res Lett* 83(1):59–66
- Kumar N, Sharma J, Arora BR, Mukopadhyay S (2009) Seismotectonic model of the Kangra-Chamba sector of Northwest Himalaya: constraints from joint hypocenter determination and focal mechanism. *Bull Seism Soc Am* 99:95–109
- Lermo J, Chavez-Garcia FJ (1993) Site effect evaluation using spectral ratios with only one station. *Bull Seism Soc Am* 83:1574–1594
- Liang X, Zhou S, Chen YJ, Jin G, Xiao L, Liu P, Fu Y, Tang Y, Lou X, Ning J (2008) Earthquake distribution in Southern Tibet and its tectonic implications. *J Geophys Res* 113(B12409):11. doi:10.1029/2007JB005101
- Loukachev I, Pralle N, Gudehus G (2002) Dilatancy-induced P waves as evidence for nonlinear soil behavior. *Bull Seism Soc Am* 92:854–862
- Mittal H, Kumar A (2015) Stochastic finite-fault modeling of Mw 5.4 earthquake along Uttarakhand–Nepal border. *Nat Hazards* 75(2):1145–1166
- Mittal H, Kamal K, Kumar A, Singh SK (2013a) Estimation of site effects in Delhi using standard spectral ratio. *Soil Dyn Earthq Eng* 50:53–61

- Mittal H, Kumar A, Kamal (2013b) Ground motion estimation in Delhi from postulated regional and local earthquakes. *J Seismol* 17(2): 593–605
- Mittal H, Kumar A, Kumar A (2013c) Site effects estimation in Delhi from the Indian strong motion instrumentation network. *Seismol Res Lett* 84(1):33–41
- Mittal H, Kumar A, Ramhmachhuani R (2012) Indian national strong motion instrumentation network and site characterization of its stations. *Int J Geosci* 3(6):1151–1167
- Mittal H, Kumar A, Kumar A, Kumar R (2015) Analysis of ground motion in Delhi from earthquakes recorded by strong motion network. *Arab J Geosci* 8(4):2005–2017
- Mittal H, Wu YM, Chen DY, Chao WA (2016) Stochastic finite modeling of ground motion for March 5, 2012, Mw 4.6 earthquake and scenario greater magnitude earthquake in the proximity of Delhi. *Nat Hazards*. doi:10.1007/s11069-016-2236-x
- Monsalve G, Sheehan A, Schulte-Pelkum V, Rajaure S, Pandey MR, Wu F (2006) Seismicity and one dimensional velocity structure of the Himalayan collision zone: earthquakes in the crust and upper mantle. *J Geophys Res* 111:B10301. doi:10.1029/2005JB004062
- Nakamura Y (1989) A method for dynamic characteristics estimations of subsurface using microtremors on the ground surface. *QR RTRI* 30: 25–33
- Ni J, Barazangi M (1984) Seismotectonics of the himalayan collision zone: geometry of the underthrusting Indian plate beneath the Himalaya. *J Geophys Res* 89:1147–1163
- Ordaz M, Arboleda J, Singh SK (1995) A scheme of random summation of an empirical Green's function to estimate ground motions from future large earthquakes. *Bull Seism Soc Am* 85:1635–1647
- Seeber L, Armbruster JG (1981) Great detachment earthquakes along the Himalayan arc and long-term forecasting, in earthquake prediction: an international review. Maurice Ewing Series 4, American Geophysical Union, Washington, D.C., pp. 259–277
- Sharma B, Chopra S, Sutar AK, Bansal BK (2013) Estimation of strong ground motion from a great earthquake mw 8.5 in central seismic gap region, Himalaya (India) using empirical Green's function technique. *Pure Appl Geophys* 170(12):2127–2138
- Sharma B, Chopra S, Kumar V (2016) Simulation of strong ground motion for 1905 Kangra earthquake and a possible megathrust earthquake (Mw 8.5) in western Himalaya (India) using Empirical Green's Function technique. *Nat Hazards* 80(1):487–503
- Singh SK, Mohanty WK, Bansal BK, Roonwal GS (2002) Ground motion in Delhi from future large/great earthquakes in the central seismic gap of the Himalayan arc. *Bull Seism Soc Am* 92:555–569
- Singh SK, Ordaz M, Dattatrayam RS, Gupta HK (1999) A spectral analysis of the 21 May 1997, Jabalpur, India, earthquake ($M_w = 5.8$) and estimation of ground motion from future earthquakes in the Indian shield region. *Bull Seism Soc Am* 89:1620–1630
- Sokolov VY, Loh C-H, Jean W-Y (2007) Application of horizontal-to-vertical (H/V) Fourier spectral ratio for analysis of site effect on rock (NEHRP-class B) sites in Taiwan. *Soil Dynan Earthq Eng* 27:314–323
- Steidl JH, Tumarkin AG, Archuleta RJ (1996) What is a reference site? *Bull Seism Soc Am* 86:1733–1748
- Tohdo M, Hatori T, Chiba O, Takahashi K, Takemura M, Tanaka H (1995) Characteristics of vertical seismic motions and Q_p -values in sedimentary layers. *J Struct Constr Eng Trans Architectural Inst Japan* 475:45–54(in Japanese with English abstract)
- Toro G, Mcguire R (1987) An investigation into earthquake ground motion characteristics in Eastern North America. *Bull. Seism. Soc. Am.* 77:468–489
- Valdiya KS (1980) Geology of Kumaun Lesser Himalaya. Dehradun. Wadia Institute of Himalayan Geology, Dehradun, India, Interim Record, p. 291
- Wessel P, Smith WHF (1998) New improved version of generic mapping tools. *EOS Trans Am Geophys Union* 79(47):579
- Yin A (2006) Cenozoic tectonic evolution of the Himalayan orogen as constrained by along strike variation of structural geometry, exhumation history and foreland sedimentation. *Earth Sci Rev* 76:1–132